RESEARCH ARTICLE

Characterization of Phenoloxidase Activity From Spider *Polybetes pythagoricus* Hemocyanin

JOURNAL OF EXPERIMENTAL ZOOLOGY
PART A
ECOLOGICAL GENETICS AND PHYSIOLOGY
A Journal of Integrative Biology

ALDANA LAINO[1], SABRINA LAVARÍAS[2], GUSTAVO SUÁREZ[1], AGUSTINA LINO[3], AND MONICA CUNNINGHAM[1]*

[1]Instituto de Investigaciones Bioquímicas de La Plata (INIBIOLP), CCT-La Plata CONICET-Universidad Nacional de La Plata (UNLP), 60 y 120 (1900) La Plata, Argentina
[2]Instituto de Limnología de La Plata (ILPLA) CONICET CCT La Plata-UNLP, La Plata, Argentina
[3]Laboratorio de Investigación de Osteopatías y Metabolismo Mineral (LIOMM), Universidad Nacional de La Plata (UNLP), Argentina

ABSTRACT

Hemocyanin of the spider *Polybetes pythagoricus*, in addition to its typical role as an oxygen transporter, also exhibits a phenoloxidase activity induced by micellar concentrations of SDS. In the present work, we found the kinetic parameters K_m and V_{max} of *Polybetes pythagoricus* hemocyanin (*Pp*Hc) PO activity to be 0.407 mM and 0.081 μmolmin^{-1}mg protein^{-1}, respectively. Dopamine was used as the substrate with SDS at a final concentration of 10 mM and a 30-min incubation at 25°C. Conformational changes in Hc associated with the SDS treatment were analyzed using far-UV circular dichroism, intrinsic fluorescence and absorption spectroscopy. The secondary and tertiary structural changes of *Pp*Hc induced by SDS led to increases in α-helical content and tryptophan fluorescence intensity. A reduction in the absorption spectrum at 340 nm in the presence of SDS was also observed. These results suggest that the SDS-induced PO activity of *Pp*Hc can be ascribed to conformational changes in the local environment of the typer-3 copper active site. *J. Exp. Zool. 9999A: 1–9, 2015.* © 2015 Wiley Periodicals, Inc.

How to cite this article: Laino A, Lavarías S, Suárez G, Lino A, Cunningham M. 2015. Characterization of phenoloxidase activity from spider *Polybetes pythagoricus* hemocyanin. J. Exp. Zool. 9999A:1–9.

J. Exp. Zool. 9999A:1–9, 2015

Hemocyanins (Hcs) are extracellular oxygen transport proteins that are freely dissolved in the hemolymph of several mollusks and arthropods. As extracellular oxygen carriers, Hcs are responsible for precise oxygen delivery from the respiratory organs to tissues. In arthropods, Hcs are multimeric cuproproteins that form very large molecular aggregates with molecular masses up to 8 MDa (Coates and Nairn, 2014). The subunits of Hcs have a molecular weight of 70-75 kDa and are arranged as hexamers (1 × 6) or multiples of hexamers (2 × 6, 4 × 6, 6 × 6, 8 × 6). The native aggregation level is species-specific; e.g., in arachnids, Hc is organized in dihexamers or tetrahexamers (Markl, '86; Markl and Decker, '92; Voit et al., 2000). Hcs belong to a protein superfamily including phenoloxidases (POs) (E.C. 1.10.3.1), insect hexamerins, crustacean cryptocyanins and diptera hexamerin receptors, all of which possess different functions (Burmester and Scheller, '96; Soderhall and Cerenius, '98; Terwilliger et al., '99). Studies show that arthropod Hcs not only transport oxygen but also have other properties or functions, such as buffers, osmolytes

Grant sponsor: Consejo Nacional de Investigaciones Científicas y Técnicas; grant number: CONICET-PIP No. 075; grant sponsor: Agencia Nacional de Promoción Científica y Tecnológica; grant number: PICT no. 2010-1270.

*Correspondence to: Dr. Mónica Cunningham, INIBIOLP, Facultad de Ciencias Médicas, UNLP. Calle 60 y 120, La Plata (1900), Argentina.
E-mail: cunninghammoni@gmail.com

Received 18 March 2015; Revised 4 May 2015; Accepted 6 May 2015
DOI: 10.1002/jez.1947
Published online XX Month Year in Wiley Online Library (wileyonlinelibrary.com).

(Paul and Pirow, '98), molt hormones, lipid transporters (Hall et al., '95; Jaenicke et al., '99; Cunningham et al., 2007; Laino et al., 2009) and pathogen defense (Riciluca et al., 2012; Coates and Nairn, 2014).

POs are involved in several invertebrate processes, such as melanin synthesis (Soderhall and Cerenius, '98; Sugumaran, 2002; Zhuang et al., 2015; Plonka and Grabacka, 2006), immune response (Coates and Nairn, 2014) and sclerotization (Sugumaran et al., '91). Whereas Hcs transport dioxygen, POs are able to catalyze the o-hydroxylation of monophenols to o-diphenols (tyrosinase or monophenoloxidase activity), the subsequent oxidation of o-diphenols to o-quinones (catecholase or diphenoloxidase activity) or both (tyrosinases) (Decker et al., 2000; Itoh and Fukuzumi, 2007; Baird et al., 2007). However, several studies have shown that Hcs also have a PO function (Decker and Rimke, '98; Decker et al., 2001; Baird et al., 2007; Jaenicke and Decker, 2008). Although POs are found in almost every organism, recent studies on chelicerates suggest that these animals lack PO proteins and that any required PO activity is performed by Hcs (Terwilliger and Ryan, 2006). This activity would involve the conversion of Hc from an oxygen carrier to an enzymatic PO (Nagai and Kawabata, 2000; Terwilliger and Ryan, 2006). Therefore, PO activity can be induced in Hcs as in POs by in vitro activation (Lee et al., 2004; Baird et al., 2007; Jaenicke and Decker, 2008; Idakieva et al., 2013). Sodium dodecyl sulfate (SDS), commonly known as a denaturant, has been used for decades in assays to detect protein PO activity. In this process, inactive PO (Moore and Flurkey, '90; Kanade et al., 2006; Marusek et al., 2006) is converted into a functionally active PO by incubation with SDS at a concentration above the critical micelle concentration (CMC) (Baird et al., 2007; Jaenicke and Decker, 2008). In recent years, weak PO activity has been observed in Hcs of both arthropods and mollusks using this assay (Decker and Rimke, '98; Salvato et al., '98; Decker et al., 2001; Pless et al., 2003; Siddiqui et al., 2006), suggesting a dual role for Hcs. In the activation process of Hc and PO, it is assumed that the presence of SDS mimics the effects of natural activators or allosteric effectors (Nagai and Kawabata, 2000; Coates et al., 2011, 2013) by inducing a conformational switch that displaces a conserved placeholder residue (PHE49 in *Limulus* Hc) (Decker et al., 2000; Nagai et al., 2001; Baird et al., 2007; Coates et al., 2011, 2013; Coates and Nairn 2014). This conformational switch allows bulky mono-and di-phenol access to the active site (Decker et al., 2006; Coates and Nairn 2014) without denaturing the protein (Baird et al., 2007; Nillius et al., 2008).

The spider *Polybetes pythagoricus* (subphylum Chelicerata) is a nocturnal, domestic species exclusive to South America and is typically found in tropical and subtropical regions. We have performed much research on the Hc from this particular species (Cunningham et al., '94, '99; Cunningham and Pollero, '96; Laino et al., 2009). The objective of this paper is to study the different functions of the Hc from this species, including SDS-induced PO activity and to analyze the Hc conformational changes associated with SDS treatment. This is the first study performed on an Hc of a member of the Araneomorphae infraorder.

MATERIAL AND METHODS

Isolation and Purification of Polybetes pythagoricus Hemocyanin (*Pp*Hc)

A total of 25 wild specimens both male and female adults of *P. pythagoricus* were caught from barks of *Eucalyptus sp*. trees. For hemolymph collection, spiders were anesthetized with cold at 4°C for 20–30 min, and the hemolymph was collected by cardiac puncture with a 27G needle on a 1-mL syringe. Collection of hemolymph was performed in the presence of sodium citrate buffer, pH 4.6, to prevent coagulation. It was immediately centrifuged at 15,000g at 4°C for 10 min to remove the cellular fraction. The supernatant was centrifuged at 178,000g at 4°C for 22 hr (ultracentrifuge Beckman L8 70 M centrifuge with a SW 60 Ti rotor). The total volume of the tubes was fractionated from top to bottom into 0.2 mL aliquots. The protein content of each fraction was monitored spectrophotometrically at 280 nm, and a blue band corresponding to Hc presence was separated (Cunningham and Pollero, '96; Cunningham et al., '99, 2007). This band was dialyzed against stabilization buffer (100 mM Tris–HCl, containing 10 mM $CaCl_2$, 50 mM $MgCl_2$, pH 8), then it was purified by gel filtration chromatography on a Superdex 200 HR 10/30 column (Pharma, 133 Uppsala, Sweden) equilibrated and eluted with the same stabilization buffer (Cunningham and Pollero, '96). The highest peak corresponding to Hc was collected and its purity was evaluated through Native-PAGE using molecular weight standards (HMW, Pharmacia, Uppsala, Sweden), then it was concentrated with Centriprep YM-50, and dialyzed against 100 mM sodium phosphate buffer, pH 7.5.Thus it was prepared for consequential enzymatic activity assays. The 340/280 nm ratio was measured resulting in a value of 0.2, indicating the complete purification of the protein (Zlateva et al., '96; Idakieva et al., 2013).

All the manipulation and chromatographic steps were performed at 4°C. Protein concentration was determined spectrophotometrically by Lowry method (Lowry et al., '51); BSA (Sigma, St. Louis, MO, USA) was used as protein standard.

Characterization of PO Activity in Hc

PO activity measurements were performed in a total volume of 1 mL in 100 mM sodium phosphate buffer, pH 7.5, 0.3 mg/mL of Hc, with different SDS concentrations and incubated at different times, keeping a constant temperature of 25°C and using dopamine as substrate. The unstable dopamine solutions were prepared daily and kept on ice in dark to minimize auto-oxidation. Auto-oxidation of dopamine was taken away from all the determinations. We determined the optimal concentration of SDS by using 2.5–30 mM of by incubating each concentration for

5, 15, and 30 min at 25°C. We also determined the optimal temperature for PO activity. To do so, Hc was incubated at each temperature with 10 mM SDS for 30 min. The reaction started after the addition of different amounts of substrate dopamine hydrochloride (Sigma–Aldrich). PO activity was followed by monitoring a 475 nm absorbance increase due to the formation of dopachrome and its derivatives, using an ultraviolet spectrophotometer (Agilent 8453). Quartz cuvettes with a 1 cm optical path length were used. One unit is defined as the formation of 1 dopachrome μmol per minute using the absorption coefficient for dopachrome of $3600\,M^{-1}\,cm^{-1}$ at this wavelength (Munoz-Munoz et al., 2006). The absorbance value was corrected for the contribution due to the auto-oxidation of the substrate by running the same assay in the absence of protein. The reaction rate was measured from the initial quasi-linear portion of the curves (usually 0–3 min). The kinetic parameters K_m (mM) and V_{max} (μmol $min^{-1}\,mg^{-1}$) were derived from non-linear regression data analysis of the dependence of the initial rates on the substrate concentration. All assays were performed in triplicate. K_m and V_{max} values were calculated manually.

Far-UV Circular Dichroism Spectroscopy

Measurements were carried out at room temperature on a Jasco J-810 spectropolarimeter (Jasco Corporation, Japan). The instrument was calibrated with (+)-10-camphorsulfonic acid following manufacturer's instructions. Scan speed was 100 nm/min, 0.1 nm data pitch and 1 nm band width. In the far UV, 0.1 cm cells were used and protein concentration was approximately 8 mg/mL in 100 mM sodium phosphate, pH 7.5. Five scans were averaged and corrected by buffer spectrum subtraction. According to Baird et al. (2007), the CMC for SDS under these assay conditions was 1.05 mM determined by isothermal titration calorimetry and dynamic light scattering measurements. We decided to use both higher and lower concentrations of CMC of SDS. Spectra recorded in the presence of increasing concentrations of SDS (0, 0.7, 5, and 10 mM) required a 30-min incubation at 25°C prior to CD measurements.

Measurements of Intrinsic Fluorescence

Protein intrinsic fluorescence spectra were recorded on a spectrofluorometer (SLM 4800 Aminco, Urbana, IL, USA) at a 0.1 mg/mL protein concentration in 100 mM sodium phosphate buffer, pH 7.5 using 1-mL capacity quartz cuvettes. The chosen excitation wavelength was 295 nm to minimize tyrosine emission (Valpuesta et al., '87). Slit width was 4 nm for both excitation and emission. Fluorescence was measured after incubating Hc with different SDS concentrations for 30 min at 25°C. All scans were corrected by buffer spectrum subtraction. A control experiment in which SDS was added to the model compound N-acetyl-L-tryptophanamide indicated that the SDS-induced changes in Hc fluorescence were not the result of a direct interaction between the detergent and exposed tryptophan side chains in the protein, see Figure 6.

Absorption Spectroscopy

Absorption spectra of Hc samples were recorded over the range 260–380 nm. The properties of the copper binding sites were studied by monitoring the absorption peak at 340 nm, typical of type 3 copper proteins. The SDS effects on absorption spectra were determined by incubating 0.7 mg/mL Hc at 25°C, with different SDS concentrations for 30 min in 100 mM sodium phosphate buffer, pH 7.5, prior to absorption spectra measurements.

Statistical Analysis

All phenoloxidase enzyme assays were performed on three independent determinations. Results were expressed as the mean ± standard deviation (SD). Data were analyzed either by Student's *t*-test or variance analysis using Instat v.3.0. Results were considered significant at 5% level.

RESULTS

Hc Isolation and Purification

A major peak at 280 nm from chromatographic profile (corresponding to a retention time of 34.3 min) representing the Hc (which for its molecular weight could correspond to the hexameric form). Its purification was confirmed by a single band on a Native-PAGE up to the 420 kDa ladder band (Fig. 1), and then used for further analyses.

Kinetic Characterization of SDS Inducible PO Activity

SDS potential for PO activity induction in *Pp*Hc was determined using different concentrations of SDS. A direct relationship between the incubation time and PO activity induced by SDS was observed, showing the highest activity after 30 min incubation

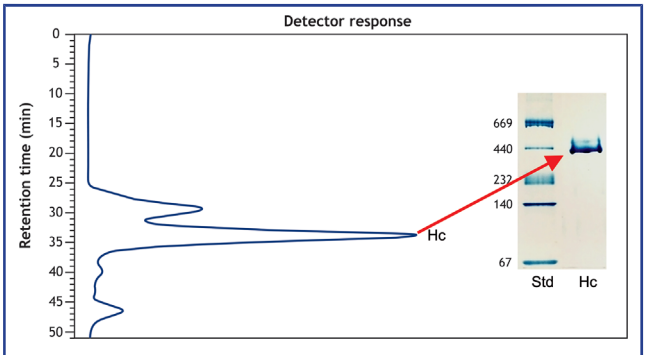

Figure 1. Chromatographic profile from FPLC obtained during purification of Hc from the *P. pythagoricus* hemolymph isolated by ultracentrifugation, on a Superdex-200 column equilibrated and eluted with 100 mM Tris–HCl, containing 10 mM $CaCl_2$, 50 mM $MgCl_2$, pH 8, at a 0.4 mL/min flow rate. The highest peak is hexamer of Hc. Inset: Native-PAGE profile of the highest peak isolated from FPLC.

(Fig. 2). PO activity was not significantly different among different concentrations of SDS at 5 and 15 min of incubation; however, after 30 min most of the activity was at 10 mM of SDS showing no significant difference between 5 and 30 mM SDS. Therefore, all subsequent results corresponded to a 30-min incubation time. Therefore, Hc displayed optimal PO activity in the presence of SDS micelles. Figure 3A–B presents the kinetic analysis of PO activity of *Pp*Hc using dopamine as substrate, final concentration of 10 mM SDS and 30-min incubation time at 25°C. The reaction followed normal Michaelis–Menten kinetics in the substrate concentration range analyzed as shown in the Lineweaver–Burk plots (Fig. 3B). The Hill coefficient value was n∼1 confirming that PO kinetics adjusts to Michaelis–Menten model. The PO apparent Michaelis–Menten constant (K_m) and V_{max} were 0.407 mM ± 0.042 and 0.081 μmol min^{-1}.mg $protein^{-1}$ ± 0.008, respectively (Fig. 3B). The K_{cat} value was 1.6 min^{-1} and the enzyme efficiency was 3.9 $mM^{-1}min^{-1}$. 1 mM dopamine was found to be the optimal concentration. Maximum PO activity was at 42°C temperature, further temperature increase did not modify PO activity (Fig. 4). Despite this we used 25°C temperature in all assays.

SDS Effect on *Pp*Hc Secondary and Tertiary Structure

Far UV CD spectra revealed a secondary structure change in *Pp*Hc when incubated at different SDS concentrations inducing an increase in α-helix content (Fig. 5). Although submicellar SDS concentrations induced a secondary structure change, more significant changes were observed at higher concentrations than that of CMC SDS.

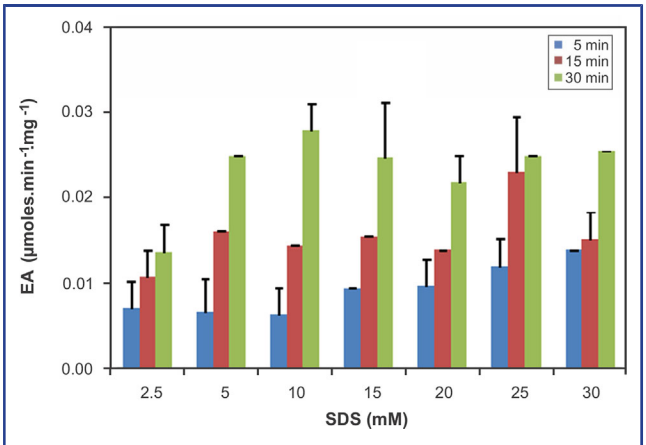

Figure 2. Effect of SDS concentration on PO activity in *P. pythagoricus*. The dependence of activation on different concentrations of SDS (2.5–30 mM; final concentrations) was assayed in 100 mM sodium phosphate buffer (pH 7.5) at 25°C. The Hc concentration was 0.3 mg/mL and 1 mM dopamine was used as substrate. First, Hc was preincubated with SDS for 5, 15, and 30 min; then the reaction was started by the addition of substrate. The reaction was followed by measuring the absorption at 475 nm.

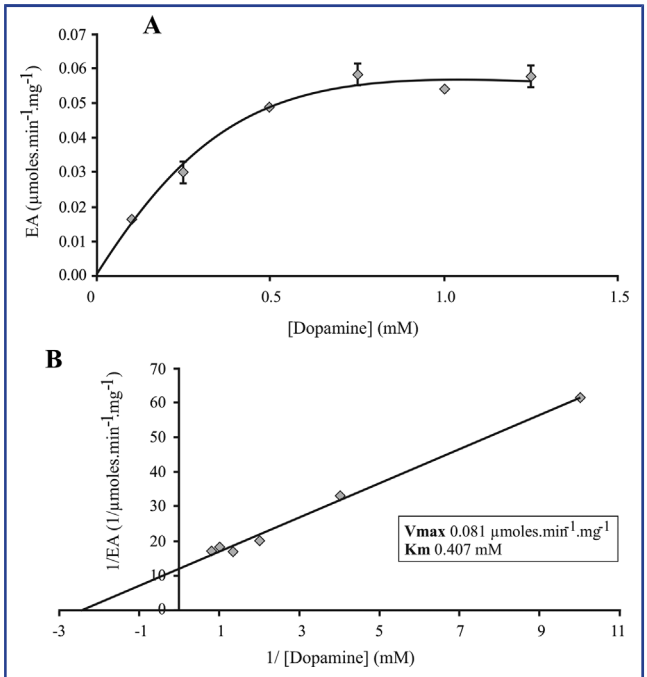

Figure 3. Kinetic analysis of PO activity in *P. pythagoricus*. **A**: The enzymatic activity of *P. pythagoricus* Hc (0.3 mg/mL) was assayed at an SDS concentration of 10 mM in 100 mM sodium phosphate buffer, pH 7.5 at 25°C. *P. pythagoricus* Hc was incubated with SDS for 30 min before addition of the dopamine substrate. **B**: Representation of Lineweaver-Burk of the effect of dopamine concentration on PO activity in *P. pythagoricus*. V_o: initial velocity. K_m: 0.407 mM, V_{max}: 0.081 μmol.min^{-1}.mg $protein^{-1}$. Hill Coefficient ∼1. Results are means ± SEM of three independent determinations.

After 30 min SDS exposure fluorescence spectra were taken showing a tryptophan fluorescence intensity increase as a result of *Pp*Hc incubation at increasing concentration of SDS (Fig. 6). Addition of submicellar SDS concentrations produced a slight change in Hc fluorescence spectra; however, SDS concentrations above CMC produced the maximum change. There was a 1.6-time total increase with respect to the control without SDS (Fig. 6, black line). We could observe that when SDS concentration increases there was a slight shift to blue in the spectrum, thus indicating that tryptophans residues are less exposed to the solvent.

Absorption Spectroscopy

In order to check the influence of SDS on the degeneration of the Cu active sites, absorption spectra of *Pp*Hc were taken at

increasing concentrations of SDS. The absorption spectrum of *Pp*Hc in 100 mM sodium phosphate buffer, pH 7.5 at 25°C, showed band with maximum at 278 nm, typical of proteins containing aromatic amino acids, and band at 340 nm due to the active site copper(II)–peroxide complex. We observed that 5 and 10 mM concentrations of SDS decreased the intensity of the copper–dioxygen band at 340 nm with the same intensity, and with 0.7 mM of SDS slightly decreased (Fig. 7). These results can be ascribed to conformational changes in the local environment of the type-3 copper active sites.

DISCUSSION

In many arthropods, PO is found in the hemolymph, hemocytes or cuticle (Cerenius and Soderhall, 2004); however, PO has not been found in chelicerata, such as scorpions, spiders and horseshoe crabs. Several studies have indicated that it is possible to convert oxygen-binding Hc into a functionally active PO (Zlateva et al., '96; Decker and Rimke, '98; Decker et al., 2001; Cerenius and Soderhall, 2004; Coates and Nairn 2014). The interaction of fatty acids and phospholipids can activate proPO (Nellaiappan and Sugumaran, '96; Bidla et al., 2009; Coates et al., 2011, 2013). SDS activation mimics this activation and is considered standard method for inducing PO activity. SDS at concentrations close to the CMC prolongs activation before complete denaturation (Baird et al., 2007; Jaenicke and Decker, 2008; Perdomo-Morales et al., 2008; Cong et al., 2009; Fan et al., 2009; Jaenicke et al., 2009; Coates et al., 2011; Idakieva et al., 2013). Generally, SDS binding during activation causes a conformational change that results in the opening of the active site, as shown for proteasomes, POs and recently for Hcs (Swain et al., '66; Dalmann et al., '85; Shibatani and Ward, '95; Kanade et al., 2006; Baird et al., 2007; Cong et al., 2009; Coates and Nairn, 2014). We examined whether *P. pythagoricus* Hc has PO activity when treated with SDS and the possible structural changes associated with this detergent addition. Absorbances between 200 and 700 nm were measured in the Hc aliquots and revealed that the 340 nm band disappeared after potassium cyanide (KCN)-treatment, indicating that this fraction contains Hc (Cunningham and Pollero, '96). The ratio between optical densities at 340 and 280 nm has been widely employed as an Hc purity criterion. In *P. pythagoricus*, the 340/280 nm ratio for purified Hc was identical to those reported in *Penaeus japonicus*, *Carcinus maenas*, *Homarus americanus* and *Cancer pagurus* (Idakieva et al., 2013). Hc hexamers are tightly interconnected structurally and are thermostable up to 80°C (Guzman-Casado et al., '90). The *E. californicum* Hc retains its structural integrity at high temperatures (Tm ~91°C) and in the presence of denaturing agents and proteases (Hubler et al., '98). *P. pythagoricus* Hc reaches maximum PO activity between 42 and 50°C, indicating relative thermostability. Nevertheless, measurements of *P. pythagoricus* PO activity were performed at 25°C, in accord with previous studies in other organisms (Jaenicke and Decker, 2008; Idakieva et al., 2009, 2013).

Dopamine is an important metabolite in sclerotization and cuticle melanization and has also been reported to be the preferred substrate of SDS-activated Hc in the tarantula *Eurypelma californicum* (Jaenicke and Decker, 2008). Due to this finding, dopamine was selected as the PO substrate. The highest observed *Pp*Hc catalytic activity was at 10 mM SDS. This phenomenon was also observed in the merostomata *Limulus polyphemus*, the scorpion *Pandinus imperator*, the spider *E. californicum* and in the crustacean *Cancer pagurus*, where half the SDS concentration and sixfold shorter incubation times were

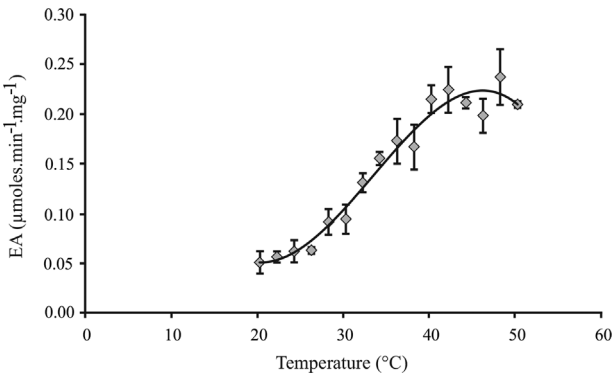

Figure 4. Effect of temperature on PO activity in *P. pythagoricus*. Values represent the mean ± one SD, n = 3.

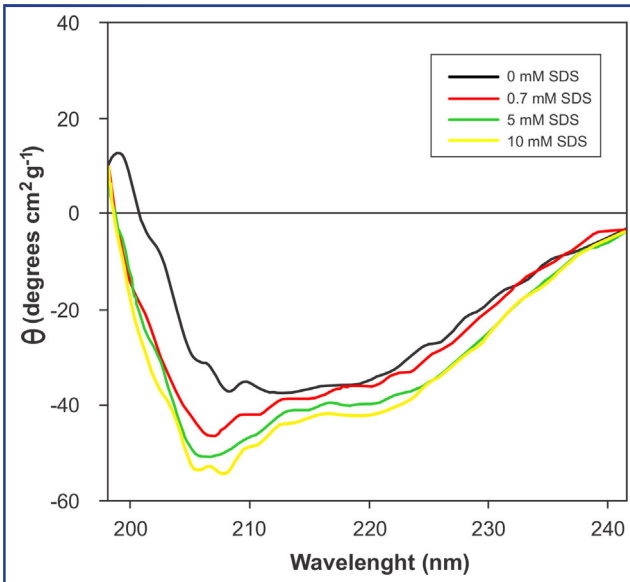

Figure 5. Far UV CD spectra of 8 mg/mL *P. pythagoricus* Hc in 100 mM sodium phosphate buffer, pH 7.5, after 30-min incubations with SDS across the range 0, 0.7 and 5 and 10 mM.

utilized (Baird et al., 2007; Jaenicke and Decker, 2008; Idakieva et al., 2013). Our results indicate that *Pp*Hc is structurally more stable than Hcs from other organisms, as it needs higher SDS concentrations and longer incubation times to achieve maximum PO activity.

Our results indicated that the *Km* of *P. pythagoricus* Hc was lower than that of *E. californicum* Hc (Jaenicke and Decker, 2008). *Pp* Hc's higher affinity for dopamine could be attributed to its hexameric structure, compared to the 24-mer of *E. californicum*; probably the conformational changes required for activation would likely leave more exposed substrate binding sites in the hexameric form. In the crustacean *Nephrops norvegicus* Hc, its dopamine hydrochloride K_m was nearly equal to that of *P. pythagoricus*, likely because both Hcs are hexameric (Coates and Nairn, 2013). However, for other crustaceans such as *Cancer pagurus*, *Panulirus argus* and *Cancer magister*, Hc K_m values were lower than those from *P. pythagoricus* and *E. californicum*, indicating that their Hcs have a greater affinity for dopamine than those of spiders (Terwilliger and Ryan, 2006; Perdomo-Morales et al., 2008; Idakieva et al., 2013). With respect to *Vmax*, our experiments showed a much slower rate when compared to the Hcs of the tarantula *E. californicum* (Jaenicke and Decker, 2008) and *L. polyphemus* (Wright et al., 2012). However, the *Vmax* of the crustacean C. *magister* Hc is the same order of magnitude as that of *P. pythagoricus* Hc, likely because they are both hexameric (Terwilliger and Ryan, 2006). K_{cat} and $K_{cat/Km}$ values were found to be higher than those in *E. californicum*, indicating that *Pp*Hc has a greater catalytic efficiency than that of *E. californicum* Hc (Terwilliger and Ryan, 2006).

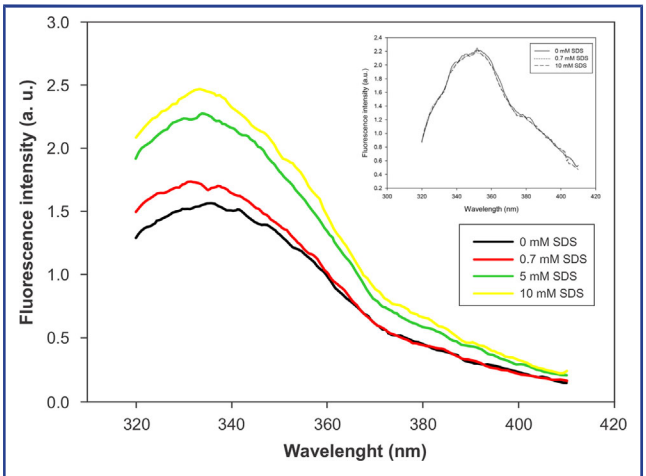

Figure 6. Fluorescence emission spectra of 0.1 mg/mL *P. pythagoricus* Hc in 100 mM sodium phosphate buffer, pH 7.5, excited at 290 nm, after 30 min incubation in SDS across the range 0, 0.7 and 5 and 10 mM. Inset: Fluorescence emission spectra of 2 μM N-acetyl tryptophan in 100 mM sodium phosphate buffer pH 7.5, excited at 290 nm, in the absence of SDS and following 30-min incubation in 0.7 mM and 10 mM SDS.

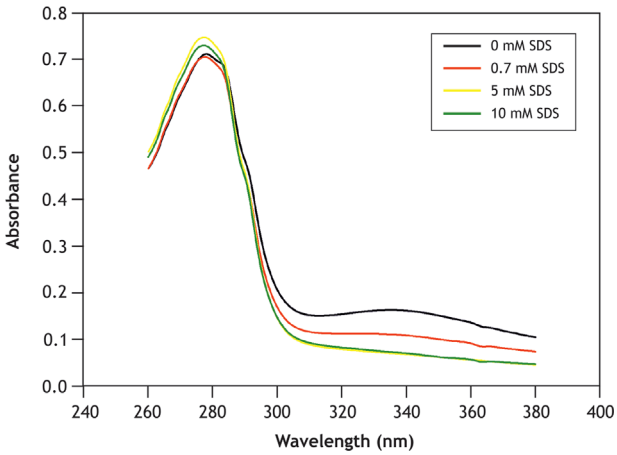

Figure 7. Absorption spectra of 0.3 mg/mL *P. pythagoricus* Hc in 100 mM sodium phosphate buffer, pH 7.5, after 30-min incubation at different concentrations of SDS (0, 0.7, 5 and 10 mM).

*Pp*Hc treated with different SDS concentrations exhibited a change in the 340 nm absorption signal, indicating structural changes close to or at the dicopper center; this effect was observed in both *L. polyphemus* and scorpion *P. imperator* Hcs, even at lower incubation times. In contrast, *E. californicum* Hc (4 × 6 form) requires a much longer incubation time (16 hr) before the characteristic copper band decrease is visible (Baird et al., 2007). The active centers in tetrahexameric *E. californicum* Hc would be less exposed than those of hexameric *P. pythagoricus* Hc.

SDS has a complex behavior when dissolved in aqueous media, as it exists as a monomer at low concentrations and forms micelles above the critical micelle concentration (Jaenicke and Decker, 2008). PO activity in Hcs is activated by SDS micelles. This activation is ascribed to enhanced substrate access to the Hc dicopper active sites at SDS concentrations above the critical micelle concentration, resulting from a conformational switch without destruction of the protein structure (Baird et al., 2007; Jaenicke and Decker, 2008). The increase in SDS-induced PO activity at concentrations above the CMC is consistent with an increase in the α-helical content of *Pp*Hc; the same logic applies to the tarantula *E. californicum* Hc, where the α-helical content increases but only after a 16-hr incubation. It is worth noting that SDS incubations above the critical micelle concentration with both spider Hcs did not lead to loss of the far-UV CD signal, indicating that no denaturation occurred. SDS-induced changes in the Hc tertiary structure were characterized by recording intrinsic fluorescence intensities. Treatment and incubation with SDS (above the CMC) led to an increase in fluorescence intensity for *Pp*Hc, likely due to changes in the microenvironment of Trp

residues and a reduction in internal quenching by the copper–dioxygen complex. This effect was also seen in fluorescence emission spectra of *L. polyphemus*, *P. imperator*, and *C. pagurus* Hcs using approximately threefold lower SDS concentrations and 6-fold shorter incubation times. In *E. californicum*, a fluorescence intensity increase was observed at half the SDS concentration and with a 32-fold longer incubation time (Baird et al., 2007; Idakieva et al., 2013). When normalized fluorescence values were observed, a blue shift was found. This observation could be attributed to the location of Trp residues in the hydrophobic region of SDS micelles. This phenomenon also occurred in the fluorescence emission maxima for *L. polyphemus* and *P. imperator*. In *E. californicum* Hc, a similar increase of fluorescence intensity occurred, although it was accompanied by a small red shift in the emission maximum. However, a 16 hr incubation with 5 mM SDS was required to elicit this response (Baird et al., 2007).

In conclusion, this is the first study performed on the Hc of a member of the Araneomorphae infraorder, in which it was shown that the spider *P. pythagoricus* Hc exhibits the properties of a common PO when it is activated by SDS. In addition to this activity, the protein exhibited changes in both its tertiary and secondary structures upon activation. Further work is necessary to establish the extent of the PO activity of *P. pythagoricus* Hc in vivo and to fully characterize the effects of PO inhibitors in vivo in Arachnids.

ACKNOWLEDGMENTS

This work was supported by grants from Consejo Nacional de Investigaciones Científicas y Técnicas (CONICET-PIP No. 075) and Agencia Nacional de Promoción Científica y Tecnológica (PICT no. 2010-1270), Argentina. M.C. and S.L. are members of CONICET, Argentina. A.L. is recipient of a fellowship from CONICET, Argentina. We are grateful to Norma Tedesco and Rosana del Cid for the revision of the English language and M. Ramos the figure design.

LITERATURE CITED

Baird S, Kelly SM, Price NC, et al. 2007. Hemocyanin conformational changes associated with SDS-induced phenol oxidase activation. Biochim Biophys Acta 1774:1380–1394.

Bidla G, Hauling T, Dushay MS, Theopold U. 2009. Activation of insect phenoloxidase after injury: endogenous versus foreign elicitors. J Innate Immun 1:301–308.

Burmester T, Scheller K. 1996. Common origin of arthropod tyrosinase, arthropod hemocyanin, insect hexamerin, and dipteran arylphorin receptor. J Mol Evol 42:713–728.

Cerenius L, Soderhall K. 2004. The prophenoloxidase-activating system in invertebrates. Immunol Rev 198:116–126.

Coates CJ, Nairn J. 2013. Hemocyanin-derived phenoloxidase activity: a contributing factor to hyperpigmentation in *Nephrops norvegicus*. Food Chem 140:361–369.

Coates CJ, Nairn J. 2014. Diverse immune functions of hemocyanins. Dev Comp Immunol 45:43–55.

Coates CJ, Kelly SM, Nairn J. 2011. Possible role of phosphatidylserine-hemocyanin interaction in the innate immune response of *Limulus polyphemus*. Dev Comp Immun 35:155–163.

Coates CJ, Whalley T, Wyman M, Nairn J. 2013. A putative link between phagocytosis-induced apoptosis and hemocyanin-derived phenoloxidase activation. Apoptosis 18:1319–1331.

Cong Y, Zhang Q, Woolford D, et al. 2009. Structural mechanism of SDS-induced enzyme activity of scorpion hemocyanin revealed by electron cryomicroscopy. Structure 17:749–758.

Cunningham M, Pollero RJ. 1996. Characterization of lipoprotein fractions with high content of hemocyanin in the hemolymphatic plasma of *Polybetes pythagoricus*. J Exp Zool 274: 275–280.

Cunningham M, Pollero RJ, Gonzalez A. 1994. Lipid circulation in spiders. Transport of phospholipids, free acids and triacylglycerols as the major lipid classes by a high-density lipoprotein fraction isolated from plasma of *Polybetes pythagoricus*. Comp Biochem Physiol B 109:333–338.

Cunningham M, Gomez C, Pollero R. 1999. Lipid binding capacity of spider hemocyanin. J Exp Zool 284:368–373.

Cunningham M, García F, Pollero RJ. 2007. Arachnid lipoproteins: Comparative aspects. Comp Biochem Physiol C 146:79–87.

Dalmann B, Rutschmann M, Kuehn L, Reinauer H. 1985. Activation of the multicatalytic proteinase from rat skeletal muscle by fatty acids or sodium dodecyl sulfate. Biochem J 321:160–166.

Decker H, Rimke T. 1998. Tarantula hemocyanin shows phenoloxidase activity. J Biol Chem 273:25889–25892.

Decker H, Dillinger R, Tuczek F. 2000. How does tyrosinase work? Recent insights from model chemistry and structural biology. Angew Chem Int Ed Engl 39:1591–1595.

Decker H, Dillinger R, Tuczek F. 2000. How does tyrosinase work? Recent insights from model chemistry and structural biology. Angew Chem Int Ed Engl 39:1591–1595.

Decker H, Ryan M, Jaenicke E, Terwilliger N. 2001. SDS-induced phenoloxidase activity of hemocyanins from *Limulus polyphemus*, *Eurypelma californicum*, and *Cancer magister*. J Biol Chem 276:17796–17799.

Decker H, Schweikardt T, Tuczek F. 2006. The first crystal structure of tyrosinase: all questions answered? Angew Chem Int Ed Engl 45:4546–4550.

Fan T, Zhang Y, Yang L, et al. 2009. Identification and characterization of a hemocyanin-derived phenoloxidase from the crab *Charybdis japonica*. Comp Biochem Physiol 152:144–149.

Guzman-Casado M, Parody-Morreale A, Mateo PL, Sanchez-Ruiz JM. 1990. Differential scanning calorimetry of lobster haemocyanin. Eur J Biochem 188:181–185.

Hall M, van Heusden MC, Soderhall K. 1995. Identification of the major lipoproteins in crayfish hemolymph as proteins involved in immune recognition and clotting. Biochem Biophys Res Commun 216:939–946.

Hubler R, Fertl B, Hellmann N, Decker H. 1998. On the stability of the 24-meric hemocyanin from *Eurypelma californicum*. Biochim Biophys Acta 1383:327–339.

Idakieva K, Siddiqui NI, Meersman F, et al. 2009. Influence of limited proteolysis, detergent treatment and lyophilization on the phenoloxidase activity of Rapana thomasiana hemocyanin. Int J Biol Macromol 45:181–187.

Idakieva K, Raynova Y, Meersman F, Gielens C. 2013. Phenoloxidase activity and thermostability of *Cancer pagurus* and *Limulus polyphemus* hemocyanin. Comp Biochem Physiol B 164:201–209.

Itoh S, Fukuzumi S. 2007. Monooxygenase activity of type 3 copper proteins. Acc Chem Res 40:592–600.

Jaenicke E, Decker H. 2008. Kinetic properties of catecholoxidase activity of tarantula hemocyanin. FEBS J 275:1518–1528.

Jaenicke E, Foll R, Decker H. 1999. Spider hemocyanin binds ecdysone and 20-OH-ecdysone. J Biol Chem 274:34267–34271.

Jaenicke E, Fraune S, May S, et al. 2009. Is activated hemocyanin instead of phenoloxidase involved in immune response in woodlice?. Dev Comp Immunol 33:1055–1063.

Kanade SR, Paul B, Rao AG, Gowda LR. 2006. The conformational state of polyphenol oxidase from field bean (*Dolichos lablab*) upon SDS and acid-pH activation. Biochem J395:551–562.

Laino A, Cunningham M, García F, Heras H. 2009. First insight into the lipid uptake, storage and mobilization in arachnids: Role of midgut diverticula and lipoproteins. J Insect Physiol 55:1118–1124.

Lee SY, Lee BL, Soderhall K. 2004. Processing of crayfish hemocyanin subunits into phenoloxidase. Biochem Biophys Res Commun 322:490–496.

Lowry OH, Rosenbrough NJ, Farr AL, Randall R. 1951. Protein measurement with the Folin phenol reagent. J Biol Chem 193:265–275.

Markl J, Decker H. 1992. Molecular structure of the arthropod hemocyanins. Adv Comp Env Physiol 13:325–376.

Markl J. 1986. Evolution and function of structurally diverse subunits in the respiratory protein hemocyanin from arthropods. Biol Bull 171:90–115.

Marusek CM, Trobaugh NM, Flurkey WH, Inlow JK. 2006. Comparative analysis of polyphenol oxidase from plant and fungal species. J Inorg Biochem 100:108–123.

Moore BM, Flurkey WH. 1990. Sodium dodecyl sulfate activation of a plant polyphenoloxidase. Effect of sodium dodecyl sulfate on enzymatic and physical characteristics of purified broad bean polyphenoloxidase. J Biol Chem 265:4982–4988.

Munoz-Munoz JL, Garcia-Molina F, Varon R, et al. 2006. Calculating molar absortivities for quinones: application to themeasurements of tyrosinase using 3,4-dihydroxymandelic acid. Ana Biochem 195:369–374.

Nagai T, Kawabata S. 2000. A link between blood coagulation and prophenol oxidase activation in arthropod host defense. J Biol Chem 275:29264–29267.

Nagai T, Osaki T, Kawabata S. 2001. Functional conversion of hemocyanin to phenoloxidase by horseshoe crab antimicrobial peptides. J Biol Chem 276:27166–27170.

Nellaiappan K, Sugumaran M. 1996. On the presence of prophenoloxidase in the hemolymph of the horseshoe crab, *Limulus*. Comp Biochem Physiol B 113:163–168.

Nillius D, Jaenicke E, Decker H. 2008. Switch between tyrosinase and catecholoxidase activity of scorpion hemocyanin by allosteric effectors. FEBS Lett 582:749–754.

Paul RJ, Pirow R. 1998. The physiological significance of respiratory proteins in invertebrates. Zoology 100:319–327.

Perdomo-Morales R, Montero-Alejo V, Perera E, Pardo-Ruiz Z, Alonso-Jimenez E. 2008. Hemocyanin-derived phenoloxidase activity in the spiny lobster *Panulirus argus* (Latreille, 1804). Biochim Biophys Acta 1780:652–658.

Pless DD, Aguilar MB, Falcon A, Lozano-Alvarez E, Heimer de la Cotera EP. 2003. Latent phenoloxidase activity and N-terminal amino acid sequence of hemocyanin from *Bathynomus giganteus*, a primitive crustacean. Arch Biochem Biophys 409:402–410.

Plonka PM, Grabacka M. 2006. Melanin synthesis in microorganisms-biotechnological and medical aspects. Acta Biochim Pol 53:429–443.

Riciluca KC, Sayegh RS, Melo RL, Silva PI, Jr. 2012. Rondonin an antifungal peptide from spider (*Acanthoscurria rondoniae*) haemolymph. Results Immunol 2: 66–71.

Salvato B, Santamaria M, Beltramini M, Alzuet G, Casella L. 1998. The enzymatic properties of Octopus vulgaris hemocyanin: o-diphenol oxidase activity. Biochemistry 37:14065–14077.

Shibatani T, Ward WF. 1995. Sodium dodecyl sulfate (SDS) activation of the 20S proteasome in rat liver. Arch Biochem Biophys 321:160–166.

Siddiqui NI, Akosung RF, Gielens C. 2006. Location of intrinsic and inducible phenoloxidase activity in molluscan hemocyanin. Biochem Biophys Res Commun 348:1138–1144.

Soderhall K, Cerenius L. 1998. Role of the prophenoloxidase-activating system in invertebrate immunity. Curr Opin Immunol 10:23–28.

Sugumaran M, Dali H, Semensi V. 1991. The mechanism of tyrosinase-catalysed oxidative decarboxylation of alpha-(3,4-dihydroxyphenyl)-lactic acid. Biochem J 277:849–853.

Sugumaran M. 2002. Comparative biochemistry of eumelanogenesis and the protective roles of phenoloxidase and melanin in insects. Pigment Cell Res 15:2–9.

Swain T, Mapson L, Robb DA. 1966. Activation of Vicia faba (L.) tyrosinase as effected by denaturing agents. Phytochemistry 5:469–482.

Terwilliger NB, Ryan MC. 2006. Functional and phylogenetic analyses of phenoloxidases from brachyuran (*Cancer magister*) and branchiopod (*Artemia franciscana*, *Triops longicaudatus*) *crustaceans*. Biol Bull 210:38–50.

Terwilliger NB, Dangott L, Ryan M. 1999. Cryptocyanin, a crustacean molting protein: evolutionary link with arthropod hemocyanins and insect hexamerins. Proc Natl Acad Sci USA 96:2013–2018.

Valpuesta JM, Goni FM, Macarulla JM. 1987. Tryptophan fluorescence of mitochondrial complex III reconstituted in phosphatidylcholine bilayers. Arch Biochem Biophys 257:285–292.

Voit R, Feldmaier-Fuchs G, Schweikardt T, Decker H, Burmester T. 2000. Complete sequence of the 24-mer hemocyanin of the tarantula *Eurypelma californicum*. Structure and intramolecular evolution of the subunits. J Biol Chem 275:39339–39344.

Wright J, Clark WM, Cain JA, et al. 2012. Effects of known phenoloxidase inhibitors on hemocyanin-derived phenoloxidase from *Limulus polyphemus*. Comp Biochem Physiol B 163: 303–308.

Zhuang J, Coates CJ, Zhu H, et al. 2015. Identification of candidate antimicrobial peptides derived from abalone hemocyanin. Devel Comp Immunol 49:96–102.

Zlateva T, Di MP, Salvato B, Beltramini M. 1996. The o-diphenol oxidase activity of arthropod hemocyanin. FEBS Lett 384:251–254.